Binding Properties of Two New Hemicarcerands Whose Hemicarceplexes Undergo Chemical Reactions without Guest Release[1,2]

Clark N. Eid, Jr.,[3] Carolyn B. Knobler, Dana A. Gronbeck, and Donald J. Cram*

Contribution from the Department of Chemistry and Biochemistry, University of California, 405 Hilgard Avenue, Los Angeles, California 90024-1569

Received April 25, 1994®

Abstract: New hemicarcerands **1** and **2** were prepared in 2–10 and 25% shell closure yields from tetrol **3** and $TsOCH_2C{\equiv}CCH_2OTs$, and tetrol **3** and *cis*-$ClCH_2CH{=}CHCH_2Cl$, respectively. One-to-one carceplexes **1**·1,4-$(CH_3)_2C_6H_4$, **1**·$C_6H_5CF_3$, **1**·$C_6H_5OCF_3$, **1**·$CHCl_3$, **1**·CH_2Cl_2·CH_2Cl_2, and **1**·$BrCH_2CH(CH_3)CH_2CH_3$ were formed by heating empty **1** in guest as solvent and characterized. The decomplexation rates in $CDCl_3$ of the first three complexes were measured at four temperatures to give $\Delta G^{\ddagger}$ values of 21.5, 21.9, and 23.3 kcal mol^{-1}, respectively, as well as $\Delta H^{\ddagger}$ and $\Delta S^{\ddagger}$ values. Hemicarceplexes **2**·$(CH_3)_2NCOCH_3$, **2**·$CH_3CH_2O_2CCH_3$, **2**·1,4-$(CH_3)_2C_6H_4$, and **2**·$CH_3C_6H_5$ were prepared by heating the mixture of complexes from shell closure in the desired guest as solvent. The new complexes were isolated and characterized, and their decomplexation rates were measured in $CDCl_3$. The crystal structures of **1**·$CHCl_2CHCl_2$ and **2**·$C_6H_5CH_3$ revealed that the hosts are untwisted and their interhemispheric bridges are oriented to maximize the cavity size. In the former, the guest occupies the torrid zones of the globe-shaped cavity, whereas the long axes of host and guest in the latter were roughly aligned. The O—C—C and C—C≡C bond angles in the bridges of **1**·$CHCl_2CHCl_2$ ranged from 99° to 105° and from 172° to 175°, respectively. Reduction of **1**·$CHCl_2CHCl_2$ and **1**·1,4-$(CH_3)_2C_6H_4$ with H_2-Pd/C gave **3**·$CHCl_2CHCl_2$ and **3**·1,4-$(CH_3)_2C_6H_4$, respectively.

Previous papers in this series reported the syntheses and binding properties of hemicarcerands **3**[4] and **4**[5] and crystal structures of some of their hemicarceplexes. These two systems each possess four portals composed of 26-membered rings, which connect their inside phases with external bulk phases in which both host and guest are soluble. The portals and cavities of **3** and **4** are appropriately sized to allow guests that range from CH_3CN to 1,4-$(CH_3)_2C_6H_4$ to enter and exit the inner phases of **3** and **4** at higher temperatures, but to allow the complexes to be manipulated in solution at ambient temperatures without dissociation. Hosts **3** and **4** exhibited large differences both with regard to structural recognition of guests and in the types of conformations occupied in their carceplexes. The crystal structures of **3**·guests generally possessed conformations in which the rigid polar caps were untwisted about their common polar axis, but the conformations of the $O(CH_2)_4O$ connecting groups adjusted to guest size by each chain controlling its own length.[4] In contrast, a crystal structure of **4**·guest (**4**·G) showed the polar caps twisted with respect to one another, which closed the portals and minimized the cavity size.[5] In a separate study, the *guests* of **3**·G were oxidized and reduced by reagents dissolved in the same bulk solvent.[6]

In the present paper, we report the syntheses and binding properties of **1** and **2**, which also contain 26-membered ring portals but whose respective $OCH_2C{\equiv}CCH_2O$ and *cis*-$OCH_2CH{=}CHCH_2O$ bridges possess widely different conformational constraints from one another and from **3** and **4**. (See Chart 1.) We particularly wished to learn if reactions could be carried out on the host of **1**·G without loss of guest in the process.

Results

Syntheses. The shell closures in the synthesis of **1**·G were conducted at high dilution by the reaction of tetraphenol **5**[7] (Chart 2) and 1,4-dichloro-2-butyne at 60 °C in $(CH_3)_2SO$ or $(CH_3)_2NCHO$–Cs_2CO_3 containing KI as catalyst. This procedure gave poor and variable yields of **1** (0–20%). The poor yields in these shell closures probably reflect the sensitivity of propargyl functionalities to alkyne–allene rearrangements. Substitution of 1,4-(ditosyloxy)-2-butyne for the dichloride, decreasing the temperature of the reaction to 25 °C, and substituting Rb_2CO_3 for Cs_2CO_3 gave **1** in the synthesis in more consistent yields (6.5%). The product was purified by chromatography on silica gel to give **1**·$CHCl_3$. Dichloromethane and chloroform leave and enter the inner phase of **1** at ambient temperature rapidly on the human time scale, but slowly on the ^1H NMR time scale. Even when the reaction was conducted in $(CH_3)_2NCOCH_3$, guest-solvent exchange occurred during isolation of the product.

The synthesis of **2**·G involved the shell closure of **5** with *cis*-1,4-dichloro-2-butene in $(CH_3)_2NCOCH_3$–Cs_2CO_3 at 60 °C for 5 days (high dilution). The product (**2**·G) was isolated as a 20:1 molar ratio of **2**·$CHCl_3$ to **2**·$CH_3CH_2O_2CCH_3$, guest exchange of **2**·$(CH_3)_2NCOCH_3$ having occurred during silica gel chromatography and solvent evaporation.

New hemicarceplexes were formed by heating solutions of **1**·$CHCl_3$ or **2**·$CH_3CH_2O_2CCH_3$ in potential guests as solvent at 100–135 °C. The solutions were cooled, and the new complexes were precipitated with hexane, collected, and dried (100 °C at 10^{-5} Torr for 18 h). Empty **1** was prepared by heating **1**·$CHCl_3$ in CCl_4 at 77 °C for 24 h. The molecules of this solvent are too large to enter the portal of **1**. This hemicarcerand and the hemicarceplexes were isolated by the above precipitation method. The following compounds were prepared and fully characterized: **1**; **1**·$CHCl_3$; **1**·$CHCl_2CHCl_2$; **1**·$CF_3C_6H_5$; **1**·$CF_3OC_6H_5$; **1**·1,4-$(CH_3)_2C_6H_4$; **1**·(*S*)-(+)-1-bromo-2-methylbutane; **2**·$(CH_3)_2NCOCH_3$; **2**·$CH_3CH_2O_2CCH_3$; **2**·$C_6H_5CH_3$; and **2**·1,4-$(CH_3)_2C_6H_4$.

* Abstract published in *Advance ACS Abstracts*, August 1, 1994.

(1) Host–Guest Complexation. 68.

(2) The authors warmly thank the U.S. Public Health Service for supporting Grant GM-12640.

(3) National Institutes of Health, National Research Service Award GM-13563, 1990–1992.

(4) Cram, D. J.; Blanda, M. T.; Paek, K.; Knobler, C. B. *J. Am. Chem. Soc.* **1992**, *114*, 7765–7773.

(5) Robbins, T. A.; Knobler, C. B.; Bellew, D. R.; Cram , D. J. *J. Am. Chem. Soc.* **1993**, *116*, 111–122.

(6) Robbins, T. A.; Cram, D. J. *J. Am. Chem. Soc.* **1993**, *115*, 12199.

(7) Cram, D. J.; Tanner, M. E.; Knobler, C. B. *J. Am. Chem. Soc.* **1991**, *113*, 7717–7727.

0002-7863/94/1516-8506$04.50/0

Chart 1

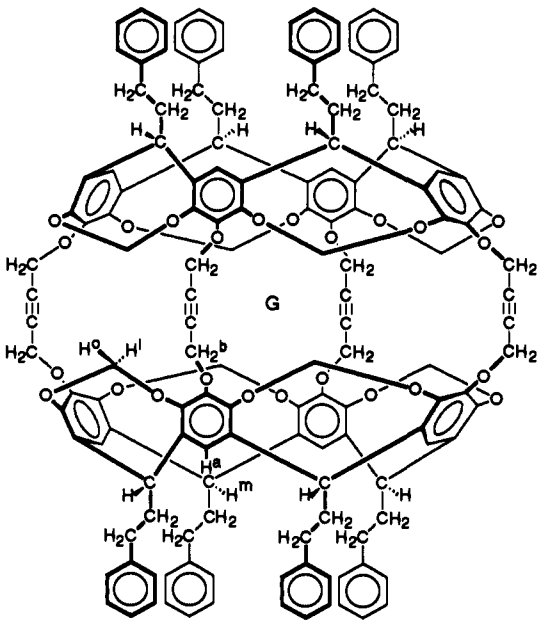

1•G

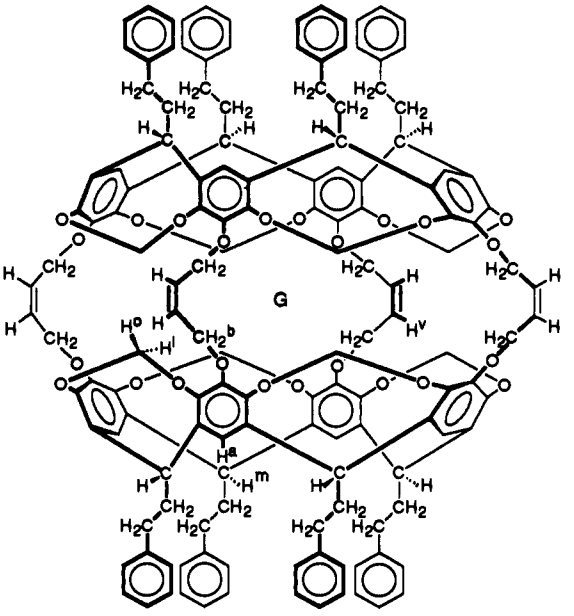

2•G

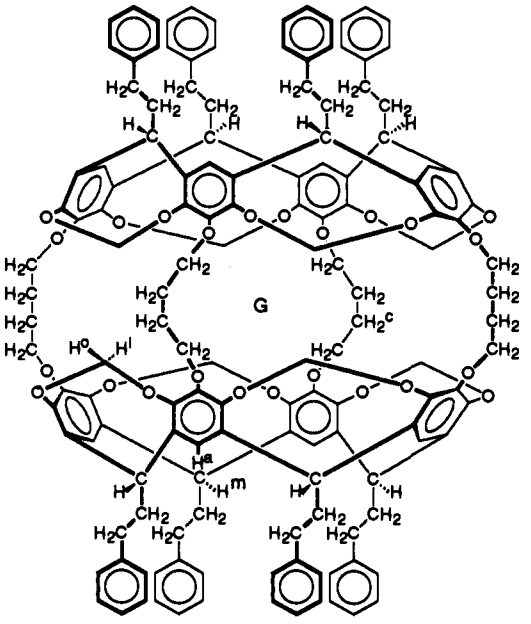

3•G

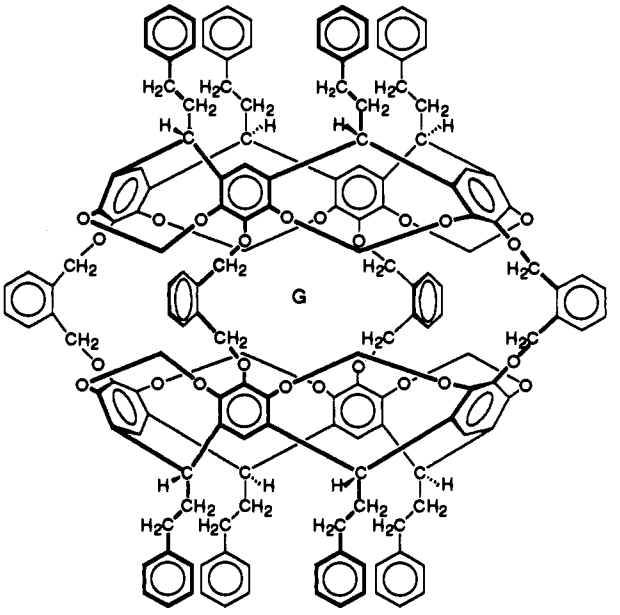

4•G

Chart 2

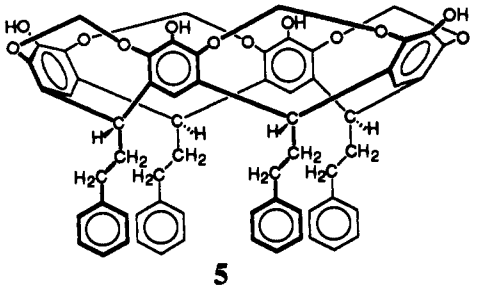

5

Attempts to isolate hemicarceplexes of **1** with the following guests failed: toluene; dichloromethane; carbon tetrachloride; 2-methyl-3-hydroxypropanoic acid, 1,4-dimethyl-2,3,5,6-tetrafluorobenzene, 1,4-bis(trifluoromethyl)benzene, 4-ethyltoluene, 1,4-diethylbenzene, adamantane, [2.2]paracyclophane, and *N*,*N*-dimethylacetamide. Hemicarcerand **2** failed to form a complex with CCl_4 or 4-ethyltoluene. Examinations of CPK models of **1** and **2** and potential guests suggest that CH_2Cl_2 goes in and out of the inner phase too easily to allow its complexes to be isolated, whereas the other guests were too large to enter the portals of **1** and **2** under the conditions employed or too large to fit into the interior of these container compounds.

When shaken in benzene solution with H_2PdC for 4 h, **1**•1,4-$(CH_3)_2C_6H_4$ and **1**•$CHCl_2CHCl_2$ gave respectively **3**•1,4-$(CH_3)_2C_6H_4$ and **3**•$CHCl_2CHCl_2$ (~80% yields) without loss of guest. The sample of **3**•1,4-$(CH_3)_2C_6H_4$ produced by this reduction was identical in its FAB MS and ^1H NMR spectra to authentic material prepared from **3** and 1,4-$(CH_3)_2C_6H_4$.[5] Complex **3**•$CHCl_2CHCl_2$ is new and was fully characterized. Attempts to synthesize **3**•$CHCl_2CHCl_2$ by heating **3** in $CHCl_2$-$CHCl_2$ at 150 °C for 3 days failed to give the complex.[5]

Spectra of Hosts, Guests, and Complexes. The 500-MHz ^1H NMR spectra of empty **1** and **2** and their complexes were examined in $CDCl_3$ at 25 °C. The chemical shifts of most of the hydrogens

Table 1. Chemical Shifts (in ppm) Relative to a Tetramethylsilane as Standard in the 500-MHz ^1H NMR Spectra in $CDCl_3$ at 25 °C of Hosts 1 and 2 and Their Complexes

structures		chemical shifts[a]						
host	guest	H^i	H^o	H^a	H^b	H^m	H^v	H^c
1	none	4.50	5.91	6.77	4.85	4.80		
1	$CDCl_3$	4.16	6.12	6.79	4.76	4.80		
1	$CHCl_2CHCl_2$	4.34	6.06	6.79	4.79	4.80		
1	$CH_3CH_2CH(CH_3)CH_2Br$	4.25	6.05	6.79	4.79	4.82		
1	$1,4\text{-}(CH_3)_2C_6H_4$	4.18	5.90	6.87	4.55	4.83		
1	$C_6H_5CF_3$	4.15	5.85	6.91	4.65	4.81		
1	$C_6H_5OCF_3$	4.23	5.85	7.11	4.64	4.81		
2	$(CH_3)_2NCOCH_3$	4.22	5.81	6.86	4.55	4.82	6.02	
2	$CH_3CH_2O_2CCH_3$	4.19[b]	5.83	6.83	4.56	4.83	6.03	
2	$1,4\text{-}(CH_3)_2C_6H_4$	4.09	5.70	6.91	4.37	4.88	6.00	
2	$C_6H_5CH_3$	4.05	5.68	6.94	4.45	4.85	6.01	
3	$CHCl_2CHCl_2$	4.37	5.79	6.80	3.92	4.80		1.95
3	$1,4\text{-}(CH_3)_2C_6H_4$	4.12	5.66	6.87	3.85	4.85		1.87

[a] See structures **1–3** for proton labels. [b] The coalescence temperature was below 25 °C, and a second signal was found at 4.12 ppm.

attached to the global parts of the hosts (labeled in **1** and **2**) changed upon complexation and are recorded in Table 1. The hydrogens attached to the 2-phenylethyl "feet" were not affected by complexation and are omitted.

Table 2 records the chemical shifts in the 500-MHz ^1H NMR and ^{19}F NMR spectra of incarcerated and free guests, as well as their differences ($\Delta\delta$) due to incarceration in hosts **1** and **2** in $CDCl_3$. Values for two guests of **3** are included for comparison.[5]

Rates and Equilibria Involving Carcerand 1. A solution of **1** in CD_2Cl_2 provided a single set of signals for the host **1**, indicating that **1**·CD_2Cl_2 was the only species present or that the complex equilibrated with **1** and CD_2Cl_2 rapidly on the ^1H NMR time scale at 25 °C to give an averaged spectrum. Interestingly, a solution of **1**·$CDCl_3$ provided 39% of **1**·$CDCl_3$ and 61% of free **1** at ambient temperature. This composition changed with temperature and was studied making use of the differences in the ^1H NMR spectral signals of free **1** and **1**·$CDCl_3$ (see Table 1). A plot of $[H\cdot CDCl_3]/([H] + [H\cdot CDCl_3])$ against temperature (K) from 294.4 to 328.3 K was reasonably linear (eight points, $R^2 = 0.978$).

The first-order decomplexation rates of **1**·G in $CDCl_3$ were measured at four convenient temperatures where G = $CF_3C_6H_5$, G = $CF_3OC_6H_5$, and G = $1,4\text{-}(CH_3)_2C_6H_4$, making use of the large difference in the ^1H NMR signals of free and incarcerated guest. Table 3 records the temperatures, half-lives, and rate constants, whereas Table 4 provides the values of the activation parameters, $\Delta H^{\ddagger}$, $\Delta S^{\ddagger}$, and $\Delta G^{\ddagger}$ at 298 K calculated from the rate constant's dependence on temperature. The mechanism of the reaction is assumed to involve dissociation of host and guest as the rate-determining step, as was demonstrated for **4**·G in a variety of solvents.[4] Qualitative observations regarding the times required for equilibrium to be reached between guest–solvent and **1**·G indicate dissociation of **1**·G to be the slow step, followed by rapid equilibration between free **1** and **1**·$CDCl_3$ for the kinetics studied in $CDCl_3$.

Crystal Structures. Crystals of **1**·$CHCl_2CHCl_2$ were grown from $C_6H_5NO_2$–$CHCl_3$ solution to give **1**·$CHCl_2CHCl_2$·$4C_6H_5NO_2$. In the crystal structure (R = 0.169) the $CHCl_2CHCl_2$ molecule is located in the inner phase. The $C_6H_5NO_2$ molecules were present as solvates, one packed between each of the four $C_6H_5CH_2CH_2$ appendages, with its nitro group facing inward, and the other two were located in adjacent regions. The host is centrosymmetric, and the $CHCl_2CHCl_2$ occupies two positions related by this center, each at half-occupancy, with their Cl atoms disordered about the three possible positions attached to their carbon atoms. Side and top stereoviews are given in **1a** and **1b**, respectively, of Chart 3, in which the $C_6H_5NO_2$ molecules located between and around the feet are omitted. The partial views along the polar axis (**1b**) of the hemicarceplex omit all of the host as well, except for the $OCH_2C{\equiv}CCH_2O$ interhemispheric bridges. In this partial structure, the four oxygens of the southern and northern hemispheres form a near-square, as shown by the heavy lines connecting each set of four oxygens. The resulting two planes are nearly parallel to one another, so that the eight oxygens approximate a cube.

Similarly, **2**·$CH_3C_6H_5$ was crystallized from $C_6H_5NO_2$–HCl_3 to give a crystal structure of **2**·$CH_3C_6H_5$·$6C_6H_5NO_2$ (R = 0.11). The host is centrosymmetric, and the guest's long axis roughly corresponds to the long axis of the host. The six $C_6H_5NO_2$

Table 2. Changes in Chemical Shifts of ^1H NMR Spectral Signals in $CDCl_3$ at 25 °C of Free and Incarcerated Guests in Hosts 1 and 2

structures			chemical shift		
		guest	free	compl.	
host	guest	atom	δ	δ	Δδ
1	$\overset{a}{C}HCl_2CHCl_2$	H^a	5.99	4.30	1.69
1	$\overset{a}{C}H_3\overset{b}{C}H_2CH(\overset{d}{C}H_3)\overset{e}{C}H_2Br$	H^a	0.89	-2.77	3.66
		H^b	1.26	1.26	1.52
		H^b	1.46	-0.68	2.14
		H^c	1.08	-0.03	1.11
		H^d	1.69	0.12	1.57
		H^e	3.30	1.40	1.90
		H^e	3.38	1.87	1.51
1	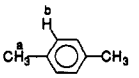	H^a	2.30	-1.66	3.96
		H^b	6.98	6.05	0.93
1	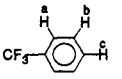	H^a	7.61	6.83	0.78
		H^b	7.54	5.61	1.93
		H^c	7.47	4.04	3.43
		F	-63.21	-63.33	0.12
1	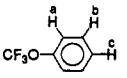	H^a	7.20	6.65	0.55
		H^b	7.39	5.42	2.15
		H^c	7.28	3.31	3.97
		F	-58.33	-60.08	1.75
2	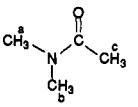	H^a	3.05	-1.51	4.56
		H^b	2.95	-0.44	3.39
		H^c	2.10	1.46	0.64
2	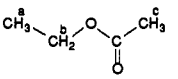	H^a	1.25	-2.08	3.33
		H^b	4.10	2.15	1.95
		H^c	2.08	-1.97	4.05
2	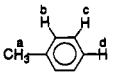	H^a	2.38	-1.57	3.95
		H^b	7.20	5.75	1.45
		H^c	7.20	5.18	2.02
		H^d	7.20	3.15	4.05
2	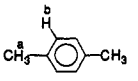	H^a	2.30	-2.00	4.30
		H^b	6.98	5.85	1.13
3	$\overset{a}{C}HCl_2CHCl_2$	H^a	5.99	4.17	1.82
3	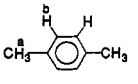	H^a	2.30	-2.10	4.20
		H^b	6.98	5.88	1.10

Table 3. First-Order Rate Constants and Half-Lives for Decomplexation of 1·G and 2·G in $CDCl_3$

complex	temp (K)	k (s^{-1}) × 10^4	R^2	half-life (h) at 318 K
1·$CF_3C_6H_5$	280	2.219	0.999	0.041[a]
	285	3.379	0.998	
	290	5.319	0.999	
	295	7.835	0.999	
1·$CF_3OC_6H_5$	280	0.455	0.999	0.027[a]
	285	1.070	0.996	
	290	1.605	0.996	
	295	4.354	0.976	
1·1,4-$(CH_3)_2C_6H_4$	313	2.504	0.996	
	318	4.152	0.999	0.46
	323	6.833	0.999	
	328	10.45	0.996	
2·1,4-$(CH_3)_2C_6H_4$	318	0.116	0.990	16.5
2·$CH_3C_6H_5$	318	*b*		vs[b]
2·$CH_3C_6H_5$	373[c]	1.80	0.991	
2·$CH_3C_6H_5$	403[c]	0.341	0.996	
2·$(CH_3)_2NCOCH_3$	318	0.750	0.988	2.6
2·$(CH_3)_2NCOCH_3$	322	0.797	0.994	
2·$(CH_3)_2NCOCH_3$	327	1.241	0.989	
2·$(CH_3)_2NCOCH_3$	332	1.475	0.996	
2·$CH_3CH_2O_2CCH_3$	318	0.411	0.987	4.7

[a] Extrapolated values. [b] The rates were too slow at 45 °C to be measured. [c] These rate constants were determined in $CDCl_2CDCl_2$.

Table 4. Activation Parameters for Decomplexation of 1·G in $CDCl_3$

	guest of 1·G			guest of 2·G
term	$CF_3C_6H_5$	$CF_3OC_6H_5$	1,4-$(CH_3)_2C_6H_4$	$(CH_3)_2NCOCH_3$
$\Delta H^{\ddagger}$ (kcal mol^{-1})	14	23	19	10
$\Delta S^{\ddagger}$ (cal mol^{-1} K^{-1})	−27	4.0	−15	−45
$\Delta G^{\ddagger}_{298}$ (kcal mol^{-1})	22	22	23	24
R^2 for k plots	1.000	0.988	1.000	0.967

molecules are located in the area of the $C_6H_5CH_2CH_2$ appendages. Side and top stereoviews are given in **2a** and **2b**. In **2a**, the $C_6H_5NO_2$ molecules are clustered between and around the feet. In the **2b** view along the long molecular axis, the $C_6H_5NO_2$ molecules and all of the host except the four *cis*-$OCH_2CH{=}CHCH_2O$ interhemispheric bridges are omitted and the two sets of four oxygens in each hemisphere are connected by lines to form two squares that are nearly parallel to one another. Table 5 lists the interesting angles and distances in **1** and **2** and includes some of the corresponding parameters of complex **3**·1,4-$(CH_3)_2C_6H_4$[5] for comparison.

Discussion

Crystal Structures. The crystal structure partial end views **1b** and **2b** show the host's hemispheres to be untwisted around their polar axes, similar to parent complexes **3**·G,[5] where guests are organic compounds, but dissimilar to those of **4**·G, whose ortho-disubstituted phenyl groups in the four bridges acquire a twist of ~21°. An examination of CPK models of **1–3** containing small guests such as CH_2Cl_2, $CHCl_3$, or CH_3CN indicates that twisting is possible and even probable since more intramolecular contacts within the host itself and intermolecular contacts between host and guest result.

A dominant feature common to all of the carcerands and hemicarcerands examined thus far that contain interhemispheric bridging groups terminated by oxygens, as in $Ar(OAO)_4Ar$, is that the unshared electron pairs of the oxygens face inward toward the cavity. This conformation minimizes the energy of the dipolar interactions arising from the three oxygens substituted in 1,2,3-positions to one another on each of the eight global aryl groups that line the hosts' cavities. The 1,3-substituted oxygens are parts of eight-membered rings, whose tightness forces the unshared electron pairs to face outward, which in turn imposes the inward-turned electron pair conformation on the middle or 2-substituent oxygen, as is observed. As a consequence, the interhemispheric bridging groups (A) are turned outward, as is visible in stereoviews **1b** and **2b**. This self-organizing feature tends to leave the inner space defined by the eight $(OAO)_4$ oxygens free of the parts of the A group.

The crystal structures of 1·$CHCl_2CHCl_2$ and 2·$CH_3C_6H_5$ provide interesting contrasts. In stereoviews **1a** and **1b**, the compact $CHCl_2CHCl_2$ guest occupies the torrid and temperate zones of the globe, an area defined mainly by the eight interhemispheric oxygens. Notice the best plane of the $CHCl_2$-$CHCl_2$ guest is tilted somewhat away from being normal to the polar axis. Notice further that all four chlorines of the guest are found close to the $CH_2C{\equiv}C$ parts of the bridging group, rather than between the bridges. This suggests the existence of attractive forces between the Cl and acetylene carbons. In 2·$CH_3C_6H_5$, the long polar axes of the host and the longest axis of the guest are nearly coincident. The methyl group and the para hydrogen of the guest extend into the opposite polar regions of the host. The other aryl hydrogens point toward the bridges, again suggesting the presence of stabilizing attractions between host and guest.

The data of Table 5 indicate the host organizations of **1**, **2**, and **3** in their complexes to be remarkably similar to one another. The largest differences are in the dihedral angles between the global aryl groups and the ArOC planes, which are 82° for **1**, ~61° for **2**, and 56° for **3**. The Ar—O—C bond angles vary from 113° in **1** to 118° in **2** and ≈104° in **3**. These variations probably reflect adaptations to the differing conformational flexibilities of the $OCH_2C{\equiv}CCH_2O$, $OCH_2CH{=}CHCH_2O$, and $O(CH_2)_4O$ connecting units. The *cavity* lengths in the polar (vertical) dimension are as follows (Å): 1·$CHCl_2CHCl_2$, 10.46; 2·$CH_3C_6H_5$, 9.61; and 3·1,4-$(CH_3)_2C_6H_4$, 9.89. The cavity (horizontal) dimensions calculated from the diagonals of the squares defined by the four oxygens in each of the interhemispheric bridges are as follows (Å): 1·$CHCl_2CHCl_2$, 5.93; 2·$CH_3C_6H_5$, 6.48; and 3·1,4-$(CH_3)_2C_6H_4$, 6.26. The longest and thicker dimensions of the three guests measured from CPK models, respectively, are as follows (Å): $CHCl_2CHCl_2$, 7.7, 4.6; $CH_3C_6H_5$, 7.7, 3.4; and 1,4-$(CH_3)_2C_6H_4$, 8.4, 3.4. Comparisons of these CPK-measured guest dimensions and the cavity sizes indicate there is plenty of room for the guests in the inner phase of the hemicarcerands provided the long axes of the host and guest are coincidental or nearly so, as in 2·$CH_3C_6H_5$ and 3·1,4-$(CH_3)_2C_6H_4$. There is not room for the guest in 1·$CHCl_2CHCl_2$ to be located with its best plane 90° to the polar axis, but there is plenty of room if the guest's best plane is tilted so this angle decreases to about 70 or 80° from the polar axis. This tilt is visible in the **1a** side view of the complex.

Notice that in the end view **1b** of the crystal structure of 1·$CHCl_2CHCl_2$, the four carbon—chlorine bonds of the guest point toward the edges of the rough cube described by the eight oxygens that terminate the four intrahemispheric bridges. This arrangement minimizes the distance between the Cl atoms of the guest and one of the two carbons of the C≡C bonds of the bridge and possibly reflects a *p–d*-orbital attractive interaction of a low order. Interestingly, the plane of the aryl guest in **2b** is roughly coincident with the best diagonal plane of the rough oxygen cube. The same thing is true in the four crystal structures reported for 3·guest[5] in which the guest is a substituted benzene ring. This type of host–guest arrangement may reflect low-order attractions of the ArH···O type.

Differences in the Portals of 1, 2, and 3. Computer drawings **6** and **7** (Chart 4) are based on the crystal structure coordinates of the host of 1·$CHCl_2CHCl_2$. The former is a ball and stick model which shows clearly the atomic attachment sequence, whereas the latter drawing closely simulates the CPK model of **1** and resembles a gazebo joined to its reflection in a pool of

Chart 3

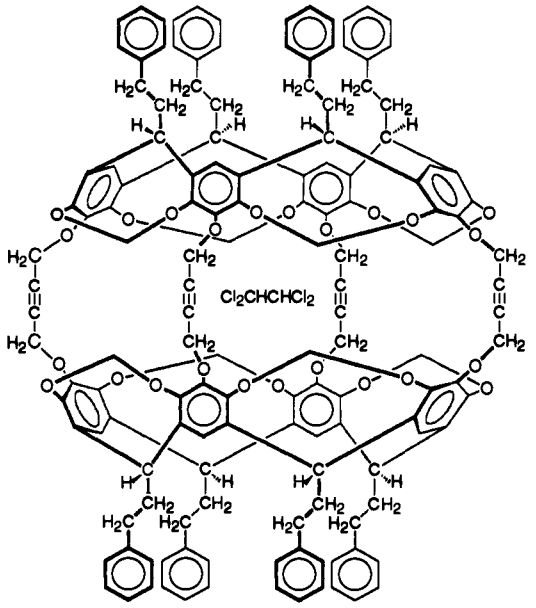

1•$CHCl_2CHCl_2$

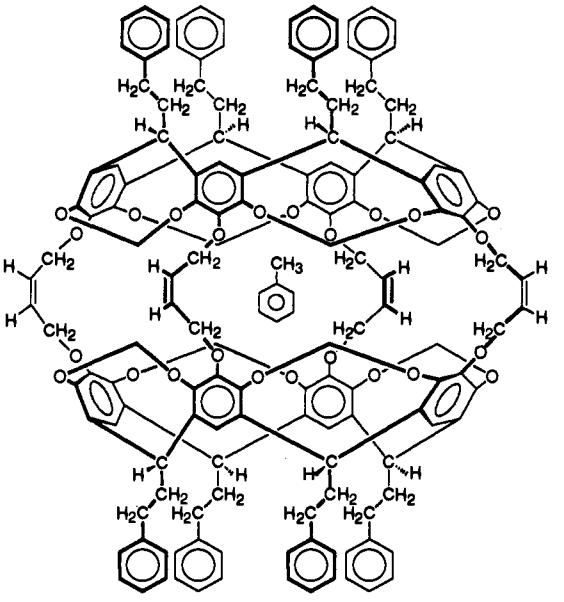

2•$CH_3C_6H_5$

Stereoviews

Stereoviews

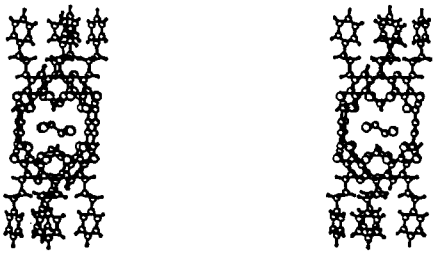

1a, side stereoview of 1•$CHCl_2CHCl_2$

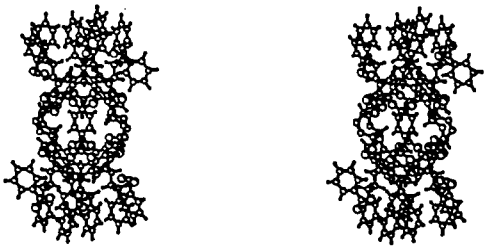

2a, side stereoview of 2•$CH_3C_6H_5$

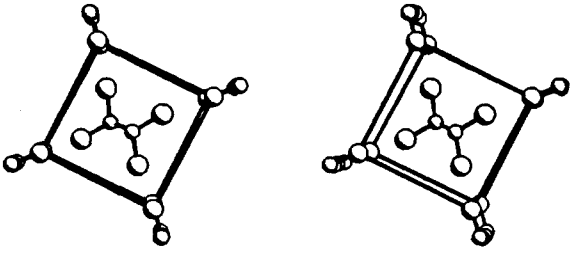

1b, end partial stereoview of 1•$CHCl_2CHCl_2$

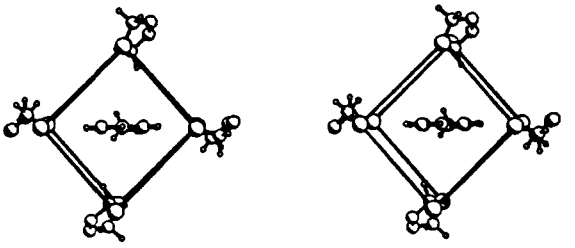

2b, end partial stereoview of 2•$CH_3C_6H_5$

water. Unlike the CPK model of **3**, the four portals of this hemicarcerand are wide apart and provide easy access and egress to guests of dimensions approaching those of these entryways. The near linearity of the $CH_2C{\equiv}CCH_2$ groups in the four interhemispheric bridges of **1** limits the range of conformational adjustments available to hosts such as **3** to adapt at high temperature to the steric requirements for guests passing into the interior of the host, and at low temperatures, blocking departure by constrictive binding. In **1**, the doors are always open, whereas in **3**, the doors can be more or less open, depending on the temperature. Accordingly, we expected the range of guests that could be captured and held in the inner phase of **3** by temperature manipulation to be larger than that for **1**. To the extent that data are available, this expectation was borne out by experiment. Thirty-five complexes of **3** were readily prepared,[5,6] whereas only five of **1** were obtained. We expect that the number formable from **2** to lie between these two numbers, but our survey of possible guests for **2** was too limited to provide any conclusions.

Chemical Shifts in the NMR Spectra of Hemicarceplexes. The effect of incarceration on the ^1H NMR spectra of guests in $CDCl_3$ of **1**•G, **2**•G, and **3**•G are compared by the $\Delta\delta$ values (δ of free guest - δ of complexed guest) of Table 2. All of the $\Delta\delta$ values in parts per million of Table 2 have positive signs, which show all of the occupiable interiors of **1** and **2** are shielded by the eight

Table 5. Interesting Host Angles (deg) and Distances (Å) in Crystal Structures of 1·$CHCl_2CHCl_2$, 2·$CH_3C_6H_5$, and 3·1,4-$(CH_3)_2C_6H_4$[a]

Angles (deg)			
complex	twist around polar axis	dihedral between Ar[a] and Ar—O—C planes	Ar—O—C[a] bond angles
1·$CHCl_2CHCl_2$	0.5	82.4 ± 0.3	113.3 ± 0.2
2·$CH_3C_6H_5$	0.5	60.7 ± 13.8	118 ± 2
3·1,4-$(CH_3)_2C_6H_4$	0	56 ± 9	104 ± 8

O—C—C—C—C—O Bridges					
		distance between best planes			
complex	distances bottom to top of C planes[b]	two central O planes	two central C planes	diagonal O—O distance[c]	OCH_2O bridges diagonal O—O distance[c]
1·$CHCl_2CHCl_2$	12.0	4.45 ± 0.01	1.19 ± 0.01	8.72 ± 0.03	9.34 ± 0.04
2·$CH_3C_6H_5$	11.15 ± 0.01	3.9 ± 0.1	1.24 ± 0.2	9.28 ± 0.30	9.38 ± 0.04
3·1,4-$(CH_3)_2C_6H_4$	11.43 ± 0.01	3.94 ± 0.01	0.45 ± 0.01	9.06 ± 0.06	9.34 ± 0.11

[a] Data on 3·1,4-$(CH_3)_2C_6H_4$ is taken from ref 5. [b] Ar-H carbons of northern and southern hemispheres. Cavity lengths are these distances minus 1.54 Å. [c] This cavity dimension is this distance minus 2.80 Å.

Chart 4

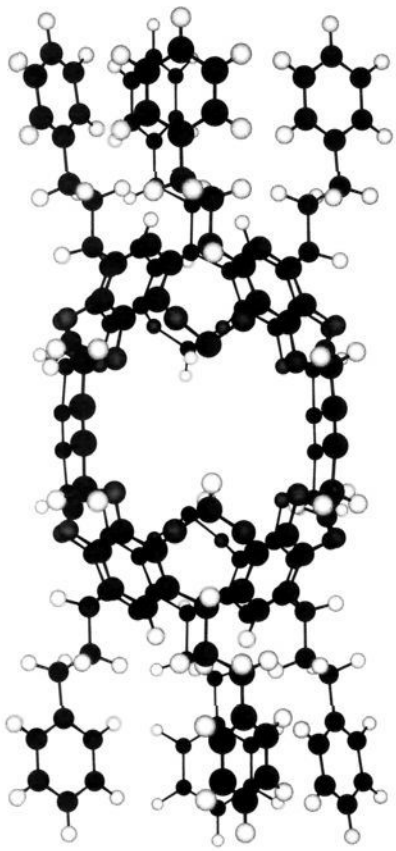

6

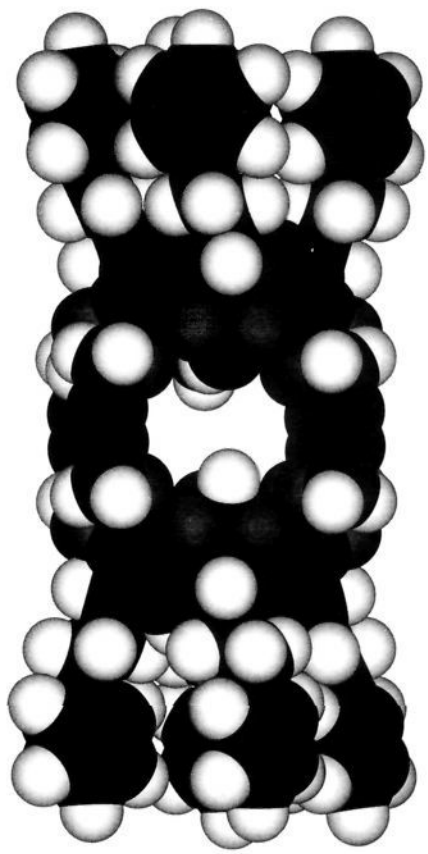

7

benzene rings that compose much of the global surfaces of the host. As expected from CPK model examination, those guest parts such as CH_3 and *p*-Ar-H, whose locations in the polar caps are the most enforced, show the highest $\Delta\delta$ values. Examples are CH_3^a of $CH_3^aCH_2CH(CH_3)CH_2Br$ in **1** ($\Delta\delta$, 3.66); CH_3^a of $CH_3^aN(CH_3)COCH_3$ in **2** ($\Delta\delta$, 4.56); and CH_3^a and CH_3^c of $CH_3^aCH_2CO_2CCH_3^c$ ($\Delta\delta$, 3.33 and 4.05, respectively). Further examples are *p*-Ar-H of 1,4-$CF_3C_6H_4H^c$ in **1** ($\Delta\delta$, 3.43); of 1,4-$CF_3OC_6H_4H^c$ in **1** ($\Delta\delta$, 3.97); and of 1,4-$CH_3C_6H_4H^b$ in **2** ($\Delta\delta$, 4.30).

A particularly interesting example involves a comparison of the $\Delta\delta$ values of the CH_3 protons in 1,4-$(CH_3)_2C_6H_4$ in **1**, **3**, and **2**, all of whose cavity lengths along the polar axes are available from crystal structure data (Tables 2 and 3 of ref 5). The respective $\Delta\delta$ values and cavity lengths in angstroms are as follows: for **1**, 3.96 and 10.48; for **3**, 4.20 and 9.89; for **2**, 4.30 and 9.61. Thus, the shorter the axial dimension of the cavity, the higher the shielding of the CH_3 protons of the 1,4-$(CH_3)_2C_6H_4$ guest, as was expected.

The lower values of $\Delta\delta$ for protons listed in Table 2 are associated with protons which must lie in the torrid region of the globe. Examples are H^c of $CH_3CH_2CH^c(CH_3)CH_2Br$ in **1** at $\Delta\delta$ = 1.11; H^b of 1,4-$(CH_3)_2C_6H_3H^b$ in **1** at $\Delta\delta$ = 0.93, in **2** at $\Delta\delta$ = 1.13, and in **3** at $\Delta\delta$ = 1.10; H^a of 1,2-$CF_3C_6H_4H^a$ in **1** at $\Delta\delta$ = 0.78; H^a of 1,2-$CF_3OC_6H_4H^a$ in **1** at $\Delta\delta$ = 0.55; and H^b of 1,2-$CH_3C_6H_4H^b$ in **2** at $\Delta\delta$ = 1.45. Examples of protons located in the temperate regions of the globe are H^a of $CH^aCl_2CHCl_2$ in **1** at $\Delta\delta$ = 1.69 and in **3** at $\Delta\delta$ = 1.82; H^b of $CH_3CH_2{}^bCH(CH_3)CH_2Br$ in **1** at $\Delta\delta$ = 1.52 and 2.14; H^b of $CH_3CH_2{}^bO_2CCH_3$ in **2** at $\Delta\delta$ = 1.95; and H^c in 1,3-$CH_3C_6H_4H^c$ in **2** at $\Delta\delta$ = 2.02.

The ^{19}F NMR signals for 1·$CF_3C_6H_5$ and 1·$CF_3OC_6H_5$

provided upfield shifts of $\Delta\delta$ = 0.12 and $\Delta\delta$ = 1.75 ppm, respectively, suggesting the fluorines are more deeply pressed into the polar cap in **1**·$CF_3OC_6H_5$, as expected. The behavior of chemical shifts of ^{19}F in shielding and deshielding environments is less well understood than the ^1H shielding–deshielding phenomenon.[8]

The chemical shifts in the ^1H NMR spectra in $CDCl_3$ of empty and guest-filled hosts **1** and **2** and two examples of **3** are listed in Table 1. As expected from CPK model examination, the eight inward-pointing H^i protons of the OCH_2O groups are generally the most guest-sensitive. In all cases, the presence of guests moved the δ values upfield from 0.45 for **2**·$C_6H_5CH_3$ to 0.13 for **3**·$CHCl_2$-$CHCl_2$. Not surprisingly, the unsaturated guests produced larger $\Delta\delta$ values than the saturated guests. Of the guests listed, all but $CH_3CH_2O_2CCH_3$ showed only one set of H^i signals at 25 °C. The other non-like-ended guests such as $(CH_3)_2NCOCH_3$, C_6H_5-CF_3, $C_6H_5OCF_3$, $C_6H_5CH_3$, and $CH_3CH_2CH(CH_3)CH_2Br$ appear to exchange their ends within the host rapidly enough on the ^1H NMR time scale to produce averaged signals. The H^i signals of **1**, **2**, and **3** in their complexes were close together, occurring at δ = 4.18, 4.09, and 4.12, respectively.

The more outward pointing protons of the OCH_2O groups (H^o) showed a less ordered sensitivity to the guests, but differed in δ as much as did H^i with host and guest change between extremes of 5.66 and 6.12 ppm. The Ar-H (H^a) and methine (H^m) protons gave δ values that varied much less than H^i and H^o with host and guest change, being more distant from the cavity and the hemispheric connecting groups of the three hosts.

Complexation of Carcerand 1 with $CDCl_3$. The complexation of $CDCl_3$ with **1** from ambient temperature to 55 °C proved to be slow on the ^1H NMR time scale, but fast on the human time scale. The composition of an equilibrated mixture in $CDCl_3$ of **1** and **1**·$CHCl_3$ changed from 35% complexed:65% uncomplexed at 17 °C to 63% complexed:37% uncomplexed at 57 °C. Thus, the *higher temperature* favors complexation, which indicates that ΔS for complexation has a positive entropy and probably makes the dominant contribution to the free energy driving force for complexation at the temperatures studied. This phenomenon was encountered previously in 1,2-$(CD_3)_2C_6D_4$ as solvent when hemicarcerand **4** complexed $C_6H_5CH_3$ at 100 °C (ΔS = 15 cal K^{-1} mol^{-1}). Although **4** also exhibited positive entropies in equilibrations with $(CH_3)_2NCOCH_3$, $CH_3CH_2O_2CCH_3$, and $CH_3COCH_2CH_3$, their $-T\Delta S$ values were smaller than their ΔH values at 100 °C.[4]

The high positive entropy for **1** binding $CDCl_3$ and **4** binding $CH_3C_6H_5$ correlates with the absence in these two guests of conformational equilibria, which could be frozen out during complexation. We interpret these unusual positive entropies as the result of two additive effects. (1) Free guest dissolved in the medium is solvated by several somewhat oriented solvent molecules, all of which must be liberated upon complexation by a single host molecule. Thus, complexation is accompanied by a net decollection of molecules. When guests that possess large flat surfaces dimerize in $CDCl_3$, ΔS values as high as 40 cal mol^{-1} K^{-1} have been observed.[9] (2) Empty hosts **1** and **4** possess inner-phase volumes considerably greater than the small empty spaces between solvent molecules. During complexation, the single large volume of the host interior becomes many small volumes between solvent molecules, thereby providing *an entropy of dilution of empty space* as one of the driving forces for complexation.

Activation Parameters for Decomplexation of 1·G in $CDCl_3$. Table 3 reports the first-order rate constants for decomplexation for three complexes of **1** and four complexes of **2** and, in favorable cases, the rate dependence on temperature. Table 4 lists the derived activation parameters for decomplexation of **1**·$CF_3C_6H_5$, **1**·$CF_3OC_6H_5$, **1**·1,4-$(CH_3)_2C_6H_4$, and **2**·$(CH_3)_2NCOCH_3$. At 45 °C in $CDCl_3$, the decomplexation half-lives *decreased* with structural changes in the following order: **1**·1,4-$(CH_3)_2C_6H_4$ > $CF_3C_6H_5$ > $CF_3OC_6H_5$, and **2**·$CH_3C_6H_5$ > **2**·1,2-$(CH_3)_2C_6H_4$ > **2**·$CH_3CH_2O_2CCH_3$ > **2**·$(CH_3)_2NCOCH_3$. The increased length and rigidity of 1,4-$(CH_3)_2C_6H_4$ combine to make it slower to decomplex **1** than either $CF_3C_6H_5$ or $CF_3OC_6H_5$. To decomplex **1** or **2**, the guests have to rotate around their short axis by ~90° to exit the host, a process resisted differentially by the inner faces of the polar caps, depending on how far the guest's ends are forced into the polar caps, and by the guest conformational flexibility. Guest $CF_3OC_6H_5$ is larger but exits faster than $CF_3C_6H_5$ because of its conformational adaptability. The spread in half-lives for decomplexation of **1** was about a power of 10. The half-lives for guest departing **2** differed by about a factor of >6. Again, the longest and most rigid guest had the longest half-life, followed by the more branched $(CH_3)_2NCOCH_3$ and less branched $CH_3CH_2OCCH_3$. In the only case studied in which the same guest exited the interior of **1** and **2**, the half-life of **2**·1,4-$(CH_3)_2C_6H_4$ > **1**·1,4-$(CH_3)_2C_6H_4$ by a factor of ~36. This result fulfills expectations based on the fact that the (OCH_2-$C{\equiv}CCH_2O$)-lined portals of **1** contain fewer space-occupying C—H bonds than the ($OCH_2CH{=}CHCH_2O$)-lined portals of **2**.

Table 4 lists the activation parameters for decomplexations of **1**·$CF_3C_6H_5$, **1**·$CF_3OC_6H_5$, **1**·1,4-$(CH_3)_2C_6H_4$, and **2**·$(CH_3)_2$-$NCOCH_3$ in $CDCl_3$. While the $\Delta G^{\ddagger}_{298}$ values of decomplexation for the three complexes of **1** were comparable at 22–23 kcal mol^{-1}, this near equality in the activation free energies is an artifact of additions of substantial $-T\Delta S^{\ddagger}$ values of 8–5 kcal mol^{-1} to dominating $\Delta H^{\ddagger}$ values of 14 and 19 kcal mol^{-1}, respectively, for **1**·$CF_3C_6H_5$ and **1**·1,4-$(CH_3)_2C_6H_4$, and the small subtraction of 1 kcal mol^{-1} for $-T\Delta S^{\ddagger}$ from the large $\Delta H^{\ddagger}$ value of 23 kcal mol^{-1} for **1**·$CF_3OC_6H_5$.

We interpret these large fluctuations in $\Delta H^{\ddagger}$ and $\Delta S^{\ddagger}$ for the decomplexation of the three complexes of **1** as follows. The activation free enthalpies (kcal mol^{-1}) decrease as follows: **1**·CF_3-OC_6H_5 (23), **1**·1,4-$(CH_3)_2C_6H_4$ (19), and **1**·$CF_3C_6H_5$ (14). This order correlates with the number and the closeness of the contacts between host and guest in the starting complexes derived from the CPK molecular model examination. Most of these stabilizing contacts must be destroyed in going to the transition states, so the transition-state enthalpies should be the highest in energy when these contacts are the more stabilizing, as is observed. The high $-T\Delta S^{\ddagger}$ values (kcal mol^{-1}) for **1**·$CF_3C_6H_5$ (8) and **1**·1,4-$(CH_3)_2C_6H_4$ (5) perhaps reflect the greater structural reorganization that the complex must undergo in its transition compared to its ground state, as compared to that for **1**·$CF_3OC_6H_5$ (−1). Both $CF_3C_6H_5$ and 1,4-$(CH_3)_2C_6H_4$ are rigidly linear molecules and to escape their prison must deform the portal, whereas CF_3-OC_6H_4 is crooked, and its shape is more adaptable to the steric requirements for occupying the portal.

Although the error in calculating $\Delta H^{\ddagger}$ and $\Delta S^{\ddagger}$ for decomplexations of **2**·$(CH_3)_2NCOCH_3$ were larger (^1H NMR signal separation problems) than those for the complexes of **1**, there is no doubt that $\Delta S^{\ddagger}$ is large and negative, and probably the $T\Delta S^{\ddagger}$ value for decomplexation of 13.4 kcal mol^{-1} at 298 K is greater than the $\Delta H^{\ddagger}$ value of 10 kcal mol^{-1}. This high entropic cost to decomplexation is in harmony with the relatively free movement of the amide guest in **2** compared to its very rigid transition state for guest exiting **2** (CPK model examination).

Reactions of Host without Loss of Guest. An interesting question to be settled is *what reactions can a carceplex undergo without losing its guests?* When submitted to the action of H_2-PdC in benzene solution, **1**·1,4-$(CH_3)_2C_6H_4$ and **1**·$CHCl_2CHCl_2$ gave (~80% yields), respectively, **3**·1,4-$(CH_3)_2C_6H_4$ and **3**·$CHCl_2$-$CHCl_2$, the former of which had been prepared by heating **3** in *p*-xylene at 138 °C for 4 days. The latter complex failed to form when a solution of **3** was heated at reflux for 3 days in $CHCl_2$-

(8) Gregory, D. H.; Glerig, J. T. *Biopolymers* **1991**, *31*, 845–858.
(9) Cram, D. J.; Choi, H. J.; Bryant, J. A.; Knobler, C. B. *J. Am. Chem. Soc.* **1992**, *114*, 7748–7765.

$CHCl_2$ as solvent.[5] The spectral properties of **3**·1,4-$(CH_3)_2C_6H_4$ prepared by the two methods were identical, whereas the FAB MS and ^1H NMR spectra and elemental analyses of **3**·$CHCl_2$-$CHCl_2$ were what were expected.

These results indicate that reactions can be carried out on the host of carceplexes without guest loss. They also illustrate how a carceplex resistant to direct formation from host and guest can be prepared by host modification of a carceplex easily formed from its components. Another study demonstrated that five new hemicarceplexes of **3** were preparable by either oxidation of incarcerated hydroquinones to incarcerated quinones or reduction of incarcerated $C_6H_5NO_2$ to incarcerated C_6H_5NHOH.[6] When added to the direct syntheses of 29 carceplexes of **3**,[5] these six indirect syntheses provide a total of 35 characterized carceplexes with **3** as host. Carcerand **3** is thus far the most broadly useful container compound we have invented and studied.

Experimental Section

General Procedures. All chemicals were reagent grade (Aldrich) and were used as obtained unless otherwise noted. Dimethylacetamide (DMA) was dried over 4-Å sieves (activated by heating to 320 °C for 24 h). A Bruker AM 500 spectrometer was used to record ^1H and ^{19}F NMR spectra. Spectra taken in $CDCl_3$ were referenced to residual $CHCl_3$ at 7.24 ppm. Mass spectra (FAB) were performed on a ZAB SE instrument, using NOBA (3-nitrobenzyl alcohol) as a matrix. Gravity chromatography was performed using E. Merck grade silica gel 60 (70–230 mesh). Thin-layer chromatography was performed on glass-backed plates (silica gel 60, F254, 0.25-mm, 1-mm, and 2-mm thicknesses).

34,47-(Epoxy[2]butynoxy)-20,24:57,61-dimethano-2,52:17,29-dimetheno-3,51,16,30-(methynoxy[2]butynoxymethyno)-1*H*,18*H*,26*H*,28*H*,53*H*,55*H*-bis[1,3]benzodioxocino[9,8-*d*:9′,8′-*d*′]bis[1,3]benzodioxocino[9′,10′:17,18;10″,9‴:25,26][1,3,6,11,14,16,19,24]octaoxacyclohexacosino[4,5-*j*:13,12-*f*′]bis[1,3]benzodioxocin, 9,10,40,41-Tetrahydro-8,11,39,42-tetrahydro-1,18,26,28,53,55,63,80-octakis(2-phenylethyl)-(1). Method A. Use of 1,4-Dichloro-2-butyne. To a 1-L round-bottom flask was added DMA (*ca.* 500 mL), and the solvent was degassed *in vacuo* for 30 min. Tetraphenol cavitand **5**[4] (1.00 g, 9.83×10^{-4} mol) and Cs_2CO_3 (11 g, 3.38 × 10^{-2} mol) were added, and the resulting suspension was heated to 60 °C under argon with stirring. To the mixture was added 1,4-dichloro-2-butyne (0.6 mL, 6.13×10^{-3} mol) in one portion by syringe. The mixture was stirred for 4 days under argon, during which time the color was observed to change from an ivory-colored suspension to a tarry brown-black suspension. The solvent was removed *in vacuo*, the residue was redissolved in $CHCl_3$, and the resulting suspension was filtered through *ca.* 25 g of Celite to remove any particulate residue. The crude material was reduced in volume to *ca.* 20 mL and chromatographed (silica/5% EtOAc in $CHCl_3$). The band with $R_f = 0.91$ was collected (this material still contained some of the brown polymeric by-product). The partially purified material was then chromatographed twice by preparative TLC (silica/$CHCl_3$). The band at $R_f = 0.59$ was isolated, extracted with 20% EtOAc in $CHCl_3$, and filtered through Celite, and the solvent was removed *in vacuo* to give **1** (41.9 mg, 1.88×10^{-5} mol, 4%) as a white solid (Note: compound **1** is isolated from the chromatogram as an equilibrium mixture of the solution-unstable $CHCl_3$ complex and empty material; the ratio of these is temperature and solvent dependent). ^1H NMR ($CDCl_3$, 500 MHz) (Note: data is given for the host at 21 °C, with 61% empty host and 39% $CDCl_3$ complex present) δ 2.42–2.47 (m, 16H, $ArCH_2CH_2$), 2.61–2.66 (m, 16H, $ArCH_2CH_2$), 4.16 (d, 8H, J = 7.31 Hz, inner CH_2-$CDCl_3$ complex), 4.50 (d, 8H, J = 7.24 Hz, inner OCH_2O-empty host), 4.76 (s, 16H, OCH_2O-$CDCl_3$ complex), 4.85 (s, 16H, OCH_2C), 4.80 (t, 8H, J = 7.90 Hz, ArCH), 5.91 (d, 8H, J = 7.23 Hz, outer OCH_2O-empty host), 6.12 (d, 8H, J = 7.18 Hz, outer OCH_2O-$CDCl_3$ complex), 6.77 (s, 8H, bowl ArH-empty host), 6.79 (s, 8H, bowl ArH-$CDCl_3$ complex), 7.10–7.13 (m, 16H, foot ArH), 7.20–7.24 (m, 24H, foot ArH); MS (Xenon FAB, NOBA matrix) *m/e* (rel int) 2234 (M^+, $C_{144}H_{120}O_{24}$, 100), 2353 (M^+, $C_{144}H_{120}O_{24}$·$CHCl_3$, 80). Purified partial $CHCl_3$ complex of **1** (20 mg, 8.95×10^{-6} mol) was dissolved in CCl_4 (10 mL). The solution was heated to reflux for 1 day in a 14/20 heavy-walled 20-mL reaction tube fitted with a condenser and inert gas inlet and then allowed to cool to 25 °C. Empty **1** was precipitated from solution by addition to *ca.* 100 mL of hexane, and the product was collected on a fine-sintered glass funnel and dried at 10^{-5} Torr, 100 °C for 10 h, to yield **1** (17 mg, 7.61×10^{-6} mol, 85%) as a white solid. Anal. Calcd for $C_{144}H_{120}O_{24}$: C, 77.40; H, 5.41. Found: C, 77.01; H, 5.49.

Method B. Use of 2-Butyne-1,4-ditosylate. The reaction was carried out in a similar fashion to that described above, using **5** (1.25 g, 1.23×10^{-3} mol), 2-butyne-1,4-di-*p*-tolunesulfonate (1.45 g, 3.69×10^{-3} mol), and Cs_2CO_3 (11 g, 3.38×10^{-2} mol) in 500 mL of degassed DMA, and was conducted at 25 °C. The reaction mixture was stirred for 8 days, and **1** was isolated in the same manner as described above except that a third preparative TLC chromatograph was necessary to yield the product (8.3 mg, 3.72×10^{-6} mol, 0.7%) as a white solid, with physical properties identical to the authentic material.

Method C. Use of Rb_2CO_3 and 2-Butyne-1,4-ditosylate. The reaction was carried out under high-dilution conditions by adding a solution of **5** (1.00 g, 9.83×10^{-4} mol) and 2-butyne-1,4-ditoluenesulfonate (1.25 g, 3.17×10^{-3} mol) in 40 mL of degassed DMA to a suspension of Rb_2CO_3 (6 g, 2.60×10^{-2} mol) in 460 mL of degassed DMA. The reaction was stirred at 25 °C for 4 days, at which time an additional portion of 2-butyne-1,4-ditoluenesulfonate (1.25 g, 3.17×10^{-3} mol) was added. Stirring was continued for an additional 4 days before performing the workup as described previously. The crude material was purified by filtration through a silica plug (using 5% EtOAc in $CHCl_3$ as eluent), followed by preparative TLC (with $CHCl_3$ as eluent). The product was isolated as described previously to yield **1** (71.0 mg, 10^{-6} mol, 6.5%) as a white solid, with physical properties identical to an authentic sample of pure host.

1·$CHCl_3$. Purified partial $CHCl_3$ complex of **1** (30 mg, 1.34×10^{-5} mol) was dissolved in $CHCl_3$ (10 mL), and the mixture was heated to reflux in a 14/20 heavy-walled 20-mL reaction tube fitted with a condenser and inert gas inlet for 10 min. Complex **1**·$CHCl_3$ was immediately precipitated from the solution by addition to *ca.* 100 mL of hexane, and the product was collected on a fine-sintered glass funnel and dried at 10^{-5} Torr, 100 °C for 10 h, to give the complex (17 mg, 7.61×10^{-6} mol, 85%) as a white solid. Anal. Calcd for $C_{144}H_{120}O_{24}$: C, 73.99; H, 5.18. Found: C, 74.16; H, 5.27.

1·$CHCl_2CHCl_2$. Purified partial $CHCl_3$ complex of **1** (50 mg, 2.24 × 10^{-5} mol) was dissolved in $CHCl_2CHCl_2$ (15 mL). The mixture was heated to reflux for 6 h in a 14/20 heavy-walled 20-mL reaction tube fitted with a condenser and inert gas inlet and allowed to cool to 25 °C. The complex was precipitated from solution by addition to *ca.* 100 mL of hexane, and the product was collected on a fine-sintered glass funnel and dried at 10^{-5} Torr, 110 °C for 18 h, to yield **1**·$CHCl_2CHCl_2$ (47 mg, 1.96×10^{-5} mol, 87%) as a white solid: ^1H NMR (500 MHz, $CDCl_3$) δ 2.37–2.49 (m, 16H, foot CH_2), 2.60–2.68 (m, 16H, foot CH_2), 4.30 (s, 2H, guest CH), 4.34 (d, 8H, J = 7.32 Hz, inner CH_2), 4.79 (s, 16H, bridge CH_2), 4.80 (t, 8H, J = 8.01 Hz, foot CH), 6.06 (d, 8H, J = 7.31 Hz, outer CH_2), 6.79 (s, 8H, bowl ArH), 7.09–7.13 (m, 16H, foot ArH), 7.17–7.24 (m, 24H, foot ArH); MS (Xenon FAB, NOBA matrix) *m/e* (rel int) 2402 (M^+, 100). Anal. Calcd for $C_{144}H_{120}O_{24}$·$CHCl_2CHCl_2$: C, 73.00; H, 5.12; Cl, 5.90. Found: C, 73.08; H, 5.12; Cl, 5.78.

1·$CF_3C_6H_5$. Purified partial $CHCl_3$ complex of **1** (18 mg, 8.23×10^{-6} mol) was dissolved in CCl_4 (2 mL), $CF_3C_6H_5$ (4 mL) was added, and the mixture was heated to reflux in a 14/20 heavy-walled 20-mL reaction tube fitted with a condenser and inert gas inlet. Within 5 min, a white precipitate had formed from the previously clear solution. The reaction was refluxed for 6 h and then allowed to cool to 25 °C. The complex was immediately precipitated from solution by addition to *ca.* 100 mL of hexane, and the product was collected on a fine-sintered glass funnel and dried at 10^{-5} Torr, 110 °C for 18 h, to yield **2**·$CF_3C_6H_5$ (14 mg, 5.80 × 10^{-6} mol, 70%) as a white solid: ^1H NMR (500 MHz, $CDCl_3$) δ 2.38–2.57 (m, 16H, foot CH_2), 2.59–2.71 (m, 16H, foot CH_2), 4.04 (t, 1H, J = 7.63 Hz, H_a of guest), 4.15 (d, 8H, J = 7.28 Hz, inner CH_2), 4.65 (s, 16H, bridge CH_2), 4.81 (t, 8H, J = 7.78 Hz, foot CH), 5.61 (t, 2H, J = 7.61 Hz, H_b of guest), 5.85 (d, 8H, J = 7.19 Hz, outer CH_2), 6.83 (d, 2H, J = 7.44 Hz, H_c of guest), 6.91 (s, 8H, bowl ArH), 7.07–7.16 (m, 16H, foot ArH), 7.16–7.24 (m, 24H, foot ArH); ^{19}F NMR (471.598 MHz, $CDCl_3$, $CFCl_3$ ref) δ_F –63.33. Anal. Calcd for C_{144}-$H_{120}O_4$·$CF_3C_6H_5$·CCl_4: C, 72.03; H, 4.97. Found: C, 72.36; H, 5.03.

1·$CF_3OC_6H_5$. Purified partial $CHCl_3$ complex of **1** (20 mg, 8.95 × 10^{-6} mol) was dissolved in CCl_4 (2 mL), $CF_3OC_6H_5$ (4 mL) was added, and the mixture was heated to reflux in a 14/20 heavy-walled 20-mL reaction tube fitted with a condenser and inert gas inlet. Within 5 min a white precipitate had formed from the previously clear solution. The reaction was refluxed for 6 h and then allowed to cool to room temperature. The complex was immediately precipitated from solution by addition to *ca.* 100 mL of hexane, and the product was collected on a fine-sintered glass funnel and dried at 10^{-5} Torr, 110 °C for 18 h, to yield **1**·$CF_3OC_6H_5$ (15 mg, 6.09×10^{-6} mol, 69%) as a white solid: ^1H NMR (500 MHz, $CDCl_3$) δ 2.38–2.56 (m, 16H, foot CH_2), 2.59–2.70 (m, 16H, foot CH_2),

3.31 (t, 1H, J = 7.75 Hz, H^a of guest), 4.23 (d, 8H, J = 7.25 Hz, inner CH_2), 4.64 (s, 16H, bridge CH_2), 4.81 (t, 8H, J = 7.95 Hz, foot CH) 5.24 (t, 2H, J = 7.79 Hz, H^b of guest), 5.85 (d, 8H, J = 7.23 Hz, outer CH_2), 6.65 (d, 2H, J = 7.97 Hz, H^c of guest), 7.01 (s, 8H, bowl ArH), 7.07–7.16 (m, 16H, foot ArH), 7.16–7.24 (m, 24H, foot ArH); ^{19}F NMR (470.598 MHz, $CDCl_3$, $CFCl_3$ ref) δ_F –60.08. Anal. Calcd for $C_{144}H_{120}O_{24}\cdot CF_3OC_6H_5$: C, 75.68; H, 5.26. Found: C, 75.44; H, 5.28.

1·*p*-Xylene. Purified partial $CHCl_3$ complex of **1** (30 mg, 1.34×10^{-5} mol) was suspended in *p*-xylene (10 mL). The mixture was heated to reflux for 6 h in a 14/20 heavy-walled 20-mL reaction tube fitted with a condenser and inert gas inlet and allowed to cool to 25 °C. The complex was precipitated from solution by addition to *ca.* 100 mL of hexane, and the product was collected on a fine-sintered glass funnel and dried at 10^{-5} Torr, 110 °C for 18 h, to yield **2**·*p*-xylene (27 mg, 1.15×10^{-5} mol, 86%) as a white solid: ^1H NMR (500 MHz, $CDCl_3$) δ –1.66 (s, 6H, guest CH_3), 2.45–2.49 (m, 16H, foot CH_2), 2.63–2.68 (m, 16H, foot CH_2), 4.18 (d, 8H, J = 7.35 Hz, inner CH_2), 4.55 (s, 16H, bridge CH_2), 4.83 (t, 8H, J = 8.00 Hz, foot CH), 5.90 (d, 8H, J = 7.32 Hz, outer CH_2), 6.05 (s, 4H, guest ArH), 6.87 (s, 8H, bowl ArH), 7.11–7.15 (m, 16H, foot ArH), 7.18–7.23 (m, 24H, foot ArH); MS (Xenon FAB, NOBA matrix) *m/e* (rel int) 2340 (M – 1, 40). Anal. Calcd for $C_{144}H_{120}O_{24}\cdot p\text{-}(1,4)_2C_6H_4$: C, 78.00; H, 5.60. Found: C, 77.86; H, 5.78.

1·(*S*)-(+)-1-Bromo-2-methylbutane. Purified partial $CHCl_3$ complex of **1** (20 mg, 8.95×10^{-6} mol) was dissolved in CCl_4 (5 mL), (*S*)-(+)-1-bromo-2-methylbutane (1 drop) was added, and the mixture was heated to reflux in a 14/20 heavy-walled 20-mL reaction tube fitted with a condenser and inert gas inlet. The reaction was refluxed for 1 day and then allowed to cool to 25 °C. The complex was precipitated from solution by addition to *ca.* 100 mL of hexane, and the product was collected on a fine-sintered glass funnel and dried at 10^{-5} Torr, 110 °C for 18 h, to give **1**·(S)-(+)-1-bromo-2-methylbutane (15 mg, 6.29×10^{-6} mol, 70%) as a white solid; ^1H NMR (500 MHz, $CDCl_3$) δ –2.77 (t, 3H, J = 7.4 Hz, guest CH_2CH_3), –0.70 (m, 1H, diastereotopic guest $CH(CH_3)CH_2CH_3$), –0.24 (m, 1H diastereotopic guest $CH(CH_3)CH_2CH_3$), –0.01 (d, 3H, J = 6.5 Hz, guest $CHCH_3$), 0.14 (m, 1H, guest $CH_2CH(CH_3)CH_2$), 1.42 (t, 1H, J = 10.0 Hz, diastereotopic guest $BrCH_2CH$), 1.89 (t, 1H, J = 10.0 Hz, diastereotopic guest $BrCH_2CH$), 2.36–2.54 (m, 16H, foot CH_2), 2.57–2.71 (m, 16H, foot CH_2), 4.27 (d, 8H, J = 7.2 Hz, inner CH_2), 4.81 (s, 16H, bridge CH_2), 4.84 (t, 8H, J = 7.9 Hz, foot CH), 6.07 (d, 8H, J = 7.2 Hz, outer CH_2), 6.81 (s, 8H, bowl ArH), 7.06–7.17 (m, 16H, foot ArH), 7.17–7.24 (m, 24H, foot ArH), MS (Xenon FAB, NOBA matrix) *m/e* (rel int) 2385 (M – 1, 56). Anal. Calcd for $C_{144}H_{120}O_{24}\cdot CH_3CH_2CH(CH_3)CH_2Br$: C, 75.02; H, 5.54; Br, 3.35. Found: C, 75.10; H, 5.34; Br, 3.27.

3·*p*-Xylene. A solution of **1**·*p*-xylene (5.3 mg, 2.26×10^{-6} mol) in benzene (50 mL) was combined with 5% Pd/C (21.4 mg) in a 250-mL pressure bottle. The mixture was attached to a Parr shaker hydrogenation apparatus, evacuated, back-filled three times with H_2, pressurized to 10 psi, and shaken for 4 h. The reaction vessel was then evacuated, the solution was filtered through Celite, and the solvent was removed *in vacuo*. The crude complex was chromatographed by preparative TLC (silica/$CHCl_3$), and the band running at R_f = 0.58 was isolated and extracted with 20% EtOAc in $CHCl_3$. The suspension was filtered, the solvent was removed, and the product was dried *in vacuo* to yield **3**·*p*-xylene (4.4 mg, 1.85×10^{-6} mol, 82%) as a white solid (Note: only ^1H NMR data are given here, as this complex was prepared by a different route and fully characterized elsewhere; the compound described here is identical in all respects to the authentic sample)[5]: ^1H NMR (500 MHz, $CDCl_3$), δ –2.10 (s, 6H, guest CH_3), 1.87 (s, 16H bridge OCH_2CH_2), 2.45–2.53 (m, 16H, foot CH_2), 2.66–2.71 (m, 16H, foot CH_2), 3.85 (s, 16H, bridge OCH_2CH_2), 4.12 (d, 8H, J = 6.97 Hz, inner CH_2), 4.85 (t, 8H, J = 7.92 Hz, foot CH), 5.66 (d, 8H, J = 7.06 Hz, outer CH_2), 5.88 (s, 4H, guest ArH), 6.87 (s, 8H, bowl ArH), 7.12–7.18 (m, 16H, foot ArH), 7.18–7.24 (m, 24H, foot ArH).

3·$CHCl_2CHCl_2$. A solution of **3**·$CHCl_2CHCl_2$ (4.8 mg, 2.00×10^{-6} mol) in benzene (50 mL) was combined with 5% Pd/C (23.0 mg) in a 250-mL pressure bottle. The mixture was attached to a Parr shaker hydrogenation apparatus, evacuated, and back-filled three times with H_2, pressurized to 10 psi, and shaken for 4 h. The reaction vessel was evacuated, the solution was filtered through Celite, and the solvent was removed *in vacuo*. The crude complex was chromatographed by preparative TLC (silica/$CHCl_3$), and the band running at R_f = 0.62 was isolated and extracted with 20% EtOAc in $CHCl_3$. The suspension was filtered, the solvent was removed, and the product was dried *in vacuo* to yield **3**·$CHCl_2CHCl_2$ (4.0 mg, 1.65×10^{-6} mol, 83%) as a white solid: ^1H NMR (500 MHz, $CDCl_3$) δ 1.95 (s, 16H, bridge OCH_2CH_2), 2.14–2.21 (m, 16H, foot CH_2), 2.62–2.69 (m, 16H, foot CH_2), 3.92 (s, 16H, bridge OCH_2CH_2), 4.17 (s, 2H, guest CH), 4.37 (d, 8H, J = 6.99 Hz, inner CH_2), 4.80 (t, 8H, J = 7.92 Hz, foot CH), 5.79 (d, 8H, J = 6.99 Hz, outer CH_2), 6.80 (s, 8H, bowl ArH), 7.12–7.17 (m, 16H, foot ArH), 7.18–7.23 (m, 24H, foot ArH); MS (Xenon FAB, NOBA matrix) *m/e* (rel int) 2417 (M^+, 100). Anal. Calcd for $C_{144}H_{136}O_{24}\cdot CHCl_2CHCl_2$: C, 72.51; H, 5.75; Cl, 5.86. Found: C, 72.81; H, 5.74; Cl, 5.46.

34,37-(Epoxy[2]butenoxy)-20,24:57,61-dimethano-2,52:17,29-dimetheno-3,51,16,30-(methynoxy[2]butenoxymethyno)-1*H*,18*H*,26*H*,53*H*,55*H*-bis[1,3]benzodioxocino[9,8-*d*:9′,8′-*d*′]bis[1,3]benzodioxocino[9′,10′:17,18;10″,9‴:25,26][1,3,6,11,14,16,19,24]octaoxacyclohexacosino[4,5-*j*:13,12-*j*′]bis[1,3]benzodioxocin, 8,11,39,42-Tetrahydro-1,18,26,28,53,55,63,80-octakis(2-phenylethyl)-, 2. 2·EtOAc and 2·$CHCl_3$ Mixture. To a Cs_2CO_3 (3.5 g) suspension of DMA (300 mL) stirred at 60 °C under argon was added over 8 h a DMA solution (60 mL) containing **5** (0.50 g, 0.50 mmol) and *cis*-1,4-dichloro-2-butene (0.32 mL, 3.0 mmol, or 1.5 equiv). After stirring for 3 days, the mixture was evaporated *in vacuo* to give a solid, which was chromatographed on silica gel with 20:1 $CHCl_3$ to EtOAc as the mobile phase to provide 139 mg (25%) of predominantly **1**·EtOAc mixed with **1**·$CHCl_3$. This mixture was converted to pure and fully characterized complexes as follows.

Complex 2·$CH_3CH_2O_2CCH_3$. An EtOAc solution (10 mL) containing mainly **2**·EtOAc (42 mg) was refluxed for 1 day. Hexane was added to precipitate the new complex, which was collected on a fine-fritted funnel and dried at 100 °C (5×10^{-5} Torr, 18 h) to give 37 mg of the EtOAc complex: ^1H NMR ($CDCl_3$, 500 MHz) δ 7.23 (m, 24H), 7.16 (m, 16H), 6.83 (s, 8H), 6.03 (bs, 8H), 5.83 (d, J = 7.2 Hz, 8H), 4.83 (bs, 8H), 4.56 (bs, 16H), 4.19 (d, J = 7.2 Hz, 4H), 4.12 (d, J = 7.2 Hz, 4H), 2.68 (m, 16H), 2.49 (m, 16H), 2.15 (G, q, J = 7.9 Hz, 2H), –1.97 (G, s, 3H), –2.08 (G, J = 7.9 Hz, 3H); see Table 1 for assignments; MS (Xenon FAB, NOBA matrix) isotope clusters at *m/e* 2331 (M + 2, 85), 2243 (M – G, 100). Anal. Calcd for $C_{144}H_{128}O_{24}\cdot CH_3CH_2O_2CCH_3$: C, 76.27; H, 5.88. Found: C, 75.89; H, 5.96.

Complex 2·$(CH_3)_2NCOCH_3$. A DMA solution (5 mL) containing 20 mg of mostly **2**·EtOAc complex was heated to 100 °C for 3 days. Hexane was added to precipitate the new complex, which was collected on a fine-fritted funnel and dried at 100 °C (5×10^{-5} Torr, 18 h) to give 15 mg of **2**·$(CH_3)_2NCOCH_3$: ^1H NMR ($CDCl_3$, 500 MHz) δ 7.24 (m, 24H), 7.16 (m, 16H), 6.86 (s, 8H), 6.02 (t, J = 3.5 Hz, 8H), 5.81 (d, J = 7.2 Hz, 8H), 4.82 (t, J = 7.9 Hz, 8H), 4.55 (d, J = 3.5 Hz, 16H), 4.22 (d, J = 7.2 Hz, 8H), 2.67 (m, 16H), 2.48 (m, 16H), 1.46 (G, s, 3H), –0.44 (G, s, 3H), –1.51 (D, s, 3H); see Table 1 for assignments; MS (Xenon FAB, NOBA matrix) isotope cluster at *m/e* 2332 (M + 2, 100). Anal. Calcd for $C_{144}H_{128}O_{24}\cdot(CH_3)_2NCOCH_3$: C, 76.30; H, 5.93; N, 0.60. Found: C, 76.14; H, 5.83; N, 0.55.

Complex 2·1,4-$(CH_3)_2C_6H_4$. A *p*-xylene solution (5 mL) containing 22 mg of mostly EtOAc complex was refluxed for 1 day. Hexane was added to precipitate the new complex, which was collected on a fine-fritted funnel and dried at 100 °C (5×10^{-5} Torr, 18 h) to give 20 mg of **2**·1,4-$(CH_3)_2C_6H_4$; ^1H NMR ($CDCl_3$, 500 MHz) δ 7.18 (m, 24H), 7.08 (m, 16H), 6.91 (s, 8H), 6.00 (t, J = 3.5 Hz, 8H), 5.85 (G, s, 4H), 5.68 (d, J = 7.2 Hz, 8H), 4.88 (t, J = 7.9 Hz, 8H), 4.37 (t, J = 3.5 Hz, 16H), 4.09 (d, J = 7.2 Hz, 8H), 2.69 (m, 16H), 2.54 (m, 16H), –2.00 (G, s, 6H); see Table 1 for assignments; MS (Xenon FAB, NOBA matrix) isotope cluster at *m/e* 2349 (M, 100). Anal. Calcd for $C_{144}H_{128}O_{24}\cdot p\text{-}(CH_3)_2C_6H_4$: C, 77.73; H, 5.92. Found: C, 77.55; H, 5.96.

Complex 2·$CH_3C_6H_5$. A toluene solution (10 mL) containing 30 mg of mostly EtOAc complex was refluxed for 18 h. The solution went from heterogeneous to homogeneous after 3 h. Hexane was added to precipitate the new carceplex, which was collected on a fine-fritted funnel and dried at 100 °C (5×10^{-5} Torr, 18 h) to give 25 mg of **2**·$CH_3C_6H_5$; ^1H NMR ($CDCl_3$, 500 MHz) δ 7.23 (m, 24H), 7.17 (m, 16H), 6.94 (s, 8H), 6.01 (t, J = 3.5 Hz, 8H), 5.75 (G, d, J = 7.1 Hz, 2H), 5.68 (d, J = 7.2 Hz, 8H), 5.18 (G, t, J = 7.1 Hz, 2H), 4.85 (t, J = 7.9 Hz, 8H), 4.45 (d, J = 3.5 Hz, 16H), 4.05 (d, J = 7.2 Hz, 8H), 3.15 (G, t, J = 7.1 Hz, 1H), 2.67 (m, 16H), 2.49 (m, 16H), –1.57 (G, s, 3H); see Table 1 for assignments; MS (Xenon FAB, NOBA matrix) isotope clusters at *m/e* 2334 (M – 1, 90), 2243 (M – G, 100). Anal. Calcd for $C_{144}H_{128}O_{24}\cdot CH_3C_6H_5$: C, 77.68; H, 5.87. Found: C, 77.47; H, 5.81.

Kinetics of Decomplexation of 1·G and 2·G. Solutions of 2–4 mg of the complex to be studied were dissolved in 0.5 mL of $CDCl_3$. The tubes were placed in the probe of the spectrometer at the desired temperature (calibrated to either methanol or ethylene glycol), and 10–18 spectra were recorded at appropriate time intervals (500-MHz spectrometer). The first-order decomplexation rate constants were calculated on the basis of spectral changes that accompanied decomplexation and are listed

in Table 1. From these parameters, ΔH°, ΔS°, and ΔG°_{298} for dissociation were calculated. The values are recorded in Table 3.

Determination of Equilibrium Compositions between 1 and 1·CDCl$_3$. Making use of the substantial δ differences in the ^{1}H NMR of empty host **1** and the host of **1**·CDCl$_3$ for H^i (see Table 1), the relative amounts of **1** and **1**·CDCl$_3$ were measured as a function of temperature over the range from 21 to 55 °C. Eight evenly dispersed points of [**1**·CDCl$_3$]/([**1**·CDCl$_3$] + [**1**]) vs temperature provided a straight line with no trends with $R^2 = 0.978$.

Crystal Structure Determinations. Complex **1**·CHCl$_2$CHCl$_2$·4C$_6$H$_5$NO$_2$ crystallized from C$_6$H$_5$NO$_2$ as colorless parallelepipeds in the monoclinic system $C2/c$. Unit cell dimensions are as follows: a = 25.786(2) Å, b = 19.862(2) Å, c = 29.240(3) Å, β = 94.956(3)°, V = 14919 Å^3, Z = 4. The crystal was examined on a modified Syntex $P\bar{1}$ diffractometer, Cu Kα radiation, at 298 K. The structure was determined by direct methods. Refinement of 245 + 77 parameters (2 blocks, 2944 reflections with $I > 3\sigma(I)$, 7655 unique reflections) has an agreement value, R, currently at 0.169. The centrosymmetric host contains one molecule of CHCl$_2$CHCl$_2$ at half-occupancy in positions related by the center of symmetry and disordered to give the Cl equal occupancy in each of the three possible positions at C. The crystal contains four nitrobenzene molecules per host located in the region of the CH$_2$CH$_2$C$_6$H$_5$ groups. A notable feature of the O—CH$_2$—C≡CCH$_2$—O bridges is the O—C—C angle. These are 105(2), 103(2), 103(2), and 99(2)°. The angles involving C≡C are nearly 180° and are all bent to about the same degree (172(3), 173(3), 173(3), and 175(3)°).

Complex **2**·C$_6$H$_5$CH$_3$·6C$_6$H$_5$NO$_2$ crystallizes from CHCl$_3$/C$_6$H$_5$NO$_2$ as colorless plates in the triclinic system $P\bar{1}$. Unit cell dimensions are as follows: a = 11.871(1) Å, b = 17.419(2) Å, c = 20.145(2) Å, α = 87.263(3)°, β = 80.698(3)°, γ = 98.199(4)°, V = 3970 Å^3, Z = 1. The crystal was examined on a modified Syntex $P\bar{1}$ diffractometer, Cu Kα radiation at 25 °C. The structure was determined by direct methods. Refinement of 289 + 89 parameters (2 blocks, 2970 reflections with $I > 3\sigma(I)$, 8159 unique reflections) has an agreement value, R, currently at 0.11.

This hemicarceplex is centrosymmetric, and the methyl group of the toluene guest is located in the cavity area defined by the four O(CH$_2$)$_4$O bridges between a plane defined by four bridge terminal oxygen atoms of one bowl and another plane defined by next nearest carbon atoms (to these oxygen atoms) of each of the four butyl bridges. The crystal contains six nitrobenzene molecules per host, located in the region of the CH$_2$-CH$_2$C$_6$H$_5$ groups.